Journal of
Materials Chemistry C

Accepted Manuscript

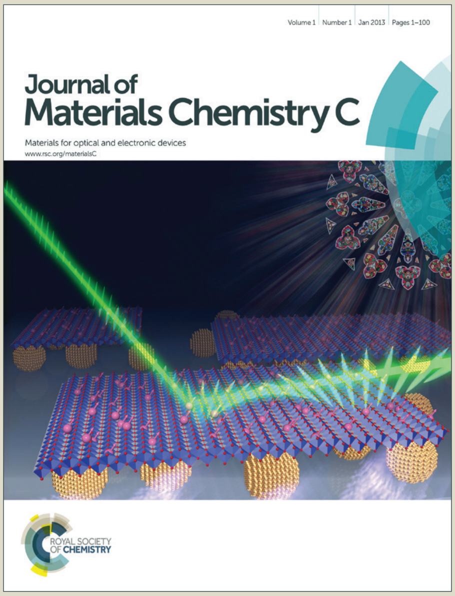

ROYAL SOCIETY
OF **CHEMISTRY**

www.rsc.org/materialsC

Journal Name RSCPublishing

COMMUNICATION

Cite this: DOI: 10.1039/x0xx00000x

Design of thermally stable rGO-embedded remote phosphor for application in white LEDs

Young-Hyun Song,[a ∇] Gill Sang Han,[a ∇] Sung Ryul Mang,[b] Mong Kwon Jung,[c] Hyun Suk Jung*[b] and Dae-Ho Yoon*[ab]

Received 00th January 2012,
Accepted 00th January 2012

DOI: 10.1039/x0xx00000x

www.rsc.org/

rGO-embedded remote phosphor was fabricated for white LEDs application. Compared with remote phosphor without rGO, rGO-embedded one showed the higher thermal quenching properties and will be expected to provide a promising candidate for new remote phosphor and the realization of white LEDs.

The introduction of white light-emitting diodes (LEDs) is a revolution in lighting technology, because of their low-power consumption, long lifetime, and high luminous efficiency, as well as their environmentally friendly properties.[1-4]. Most general lighting is based on phosphor-converted white LEDs. This type is generated by blue-emitting InGaN blue LED with yellow phosphor ($Y_3Al_5O_{12}$: Ce^{3+}). The human eye perceives white light by a combination of blue and yellow emission.[5].

However, this type of white LED using the $Y_3Al_5O_{12}$: Ce^{3+} phosphor has drawbacks in respect of thermal stress, because of the usage of encapsulants, such as silicone resins. So, the colour correlated temperature (CCT) is unstable. Remote phosphor can be an alternative for the reduction of thermal stress. However, remote phosphors using polymer-based materials for white light-emitting diodes also have several challenges from thermal stress originating from heat generation of the LEDs[6]. Instead of employing only polymer-based remote phosphor, which is susceptible to heat, thermally stable rGO with remote phosphor is adopted for the generation of white LEDs. The rGO-embedded remote phosphor is introduced as a best effective solution. Utilization of graphene sheet for the excellent performance of white LEDs gives rise to highly effective heat dissipation. Graphene has been attractive, because of its high transmittance, outstanding thermal and electrical conductivities, and flexibility.[7] In this work, we report the fabrication of highly thermally stable and rGO-embedded remote phosphor film, based on polydimethylsiloxane (PDMS). The PDMS is easy to fabricate, and has the ability to resist moisture and heat. To the best of our knowledge, a flexible remote phosphor using graphene has many advantages of bendable, non-brittle properties, compared with conventional type LEDs with heat generation by scattering light. This is the first attempt to use graphene as reinforcement in the heat dissipation of remote phosphor. Firstly, yellow-emitting $Y_3Al_5O_{12}$: Ce^{3+} phosphor was synthesized by a solid state reaction method, using the $R@B_2O_3$ ($R=Eu_2O_3$ and CeO_2) materials as an activator.[8] Graphene oxide was synthesized by a modified Hummers' method.[9] In brief, graphite was mixed with sulfuric acid and sodium nitrate. After that, potassium permanganate was slowly added into the mixture under ice bath. After 5 days of stirring, the brown mixture was washed with 5% sulfuric acid solution and water, and centrifuged. Reduced graphene oxide was prepared, with adding the hydrazine in graphene oxide solution. This solution was stirred at 90 °C for 4 hrs. After it turned black, the solution was filtered by vacuum filtration. rGO-embedded remote phosphors are prepared by a solvent exchange method. Synthesized graphene were exfoliated in ethanol with sonication. rGO was mixed with PDMS. The mixture was centrifuged at 8000 rpm for 30 min, and heated to remove ethanol. Perfectly dispersed rGO/PDMS was stirred with commercial $Y_3Al_5O_{12}$: Ce^{3+} phosphor, and then PDMS hardener was added. The ratio of PDMS to hardener was 10:1. Finally, the rGO-embedded remote phosphor was cured at 100 °C for 5 hrs. Based on the above experiments, it can be seen that the rGO-embedded remote phosphor involves the procedures, as illustrated in Figure 1.

The morphology of rGO was observed by a field-emission scanning electron microscopy (FE-SEM, JSM-7600F, JEOL). Furthermore, rGO was investigated by high-resolution transmission electron microscopy (HR-TEM, JEM-3000F, JEOL). The chemical composition of rGO-embedded PDMS was analysed using X-ray photoelectron spectroscopy (XPS-VG, Microtech ESCA 2000) and transmittance was identified by UV-visible spectroscopy (Jasco V-600 series). The crystalline phase of $Y_3Al_5O_{12}$: Ce^{3+} phosphor was identified using powder x-ray diffraction (XRD, D-MAX 2500, Rigaku) with CuKα target from $20° \leq 2\theta \leq 80°$. Optical properties of the prepared samples were analyzed by room-temperature photoluminescence spectrometry (PL, PSI Co., Ltd./Korea), equipped with a 500-W Xenon discharge lamp as an excitation source. The luminous efficiency of the phosphors was calculated using blue LEDs under 450 nm, with an integrated sphere attachment (PSI Co., Ltd./Korea). All luminescence properties of rGO-embedded remote phosphor were carried out at room temperature.

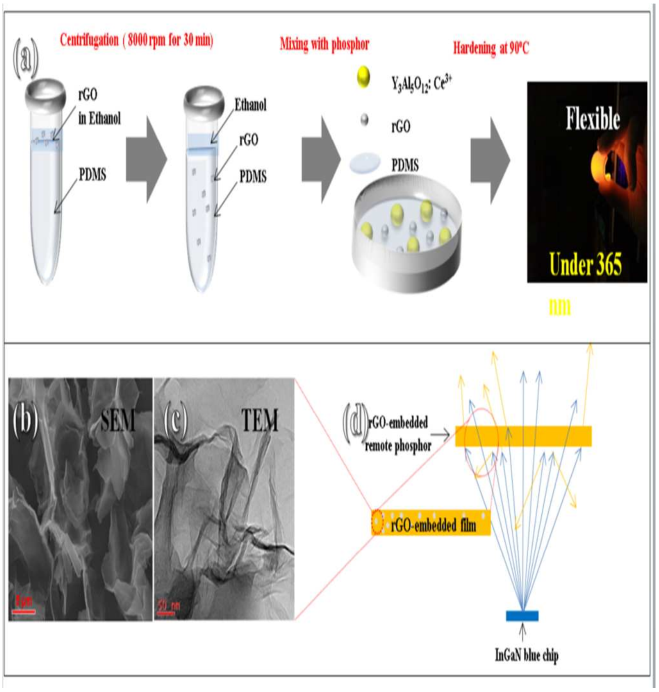

Figure 1. (a) illustration about fabrication of rGO-embedded remote phosphor, (b) SEM image of synthesized rGO, (c) TEM image of rGO, (d) scheme of rGO embedded phosphor film as white LEDs.

Figure 1 (a) shows the procedure of fabrication about rGO-embedded remote phosphor. Figure 1(b) and (c) indicate the morphology of the prepared rGO. As shown in Figure 1, typical rGO morphology is observed.

Evidence of the chemical composition of the rGO was analyzed by XPS. The C1s spectrum of rGO consists of a main component, comprising 5 peaks, as shown in Figure 2 (a). The C 1s XPS spectra of rGO indicate the presence of four types of carbon bond: C-C/C=C (284.6 eV), C-N (285.7 eV), C-O (287.3 eV), C=O (288.3 eV) and O-C=O (289.4). Figure 2 (b) shows the transmittance spectra of rGO-embedded PDMS film compared with PDMS one. High transmittance values (>76%) could be achieved in the 400 to 800 range for the two samples. The PDMS has above 3.5% transmittance in the visible region. It is very important to analyze the transmittance, because transparent materials can improve the light output and lumen maintenance.

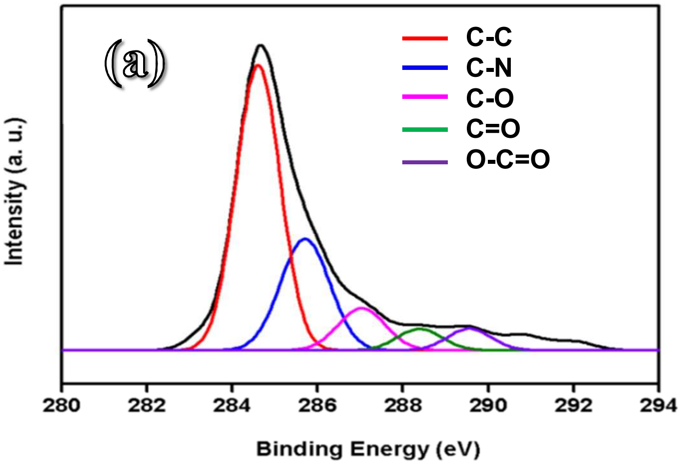

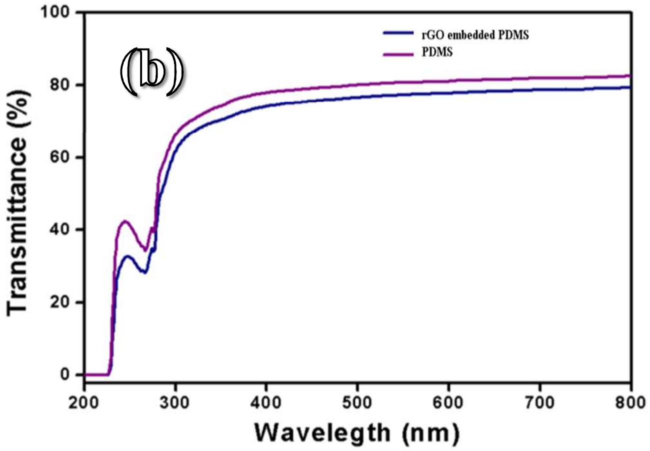

Figure 2. (a) XPS spectra the prepared rGO, (b) Transmittance spectra of rGO embedded PDMS

Figure 3 (a) indicates the XRD pattern of the prepared $Y_3Al_5O_{12}$: Ce^{3+} phosphor. The crystal structure is cubic. Crystalline single phase was obtained, which matched well the JCPDS card (33-0040). The inset of Figure 1 (a) presents a SEM image of the prepared $Y_3Al_5O_{12}$: Ce^{3+} sample, which indicates the non-aggregated morphology and well formed crystallite structure of 15 µm. The photoluminescence properties of the prepared $Y_3Al_5O_{12}$: Ce^{3+} phosphor in Figure 1(b) presents that typically broad excitation and emission band, which correspond to previous report [10].

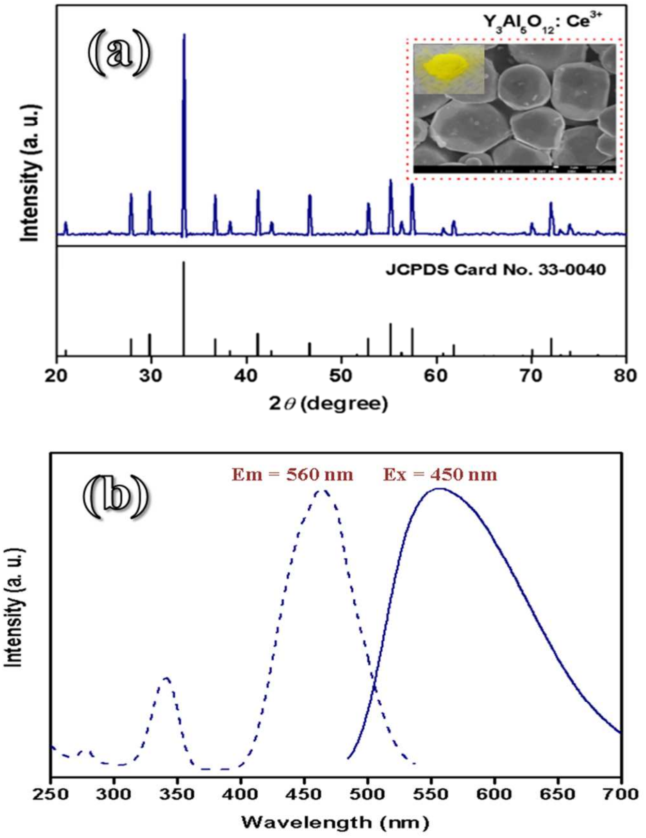

Figure 3. (a) XRD data of the synthesized $Y_3Al_5O_{12}$: Ce^{3+} sample, (b) Photoluminescence properties of yellow-emitting $Y_3Al_5O_{12}$: Ce^{3+} phosphor

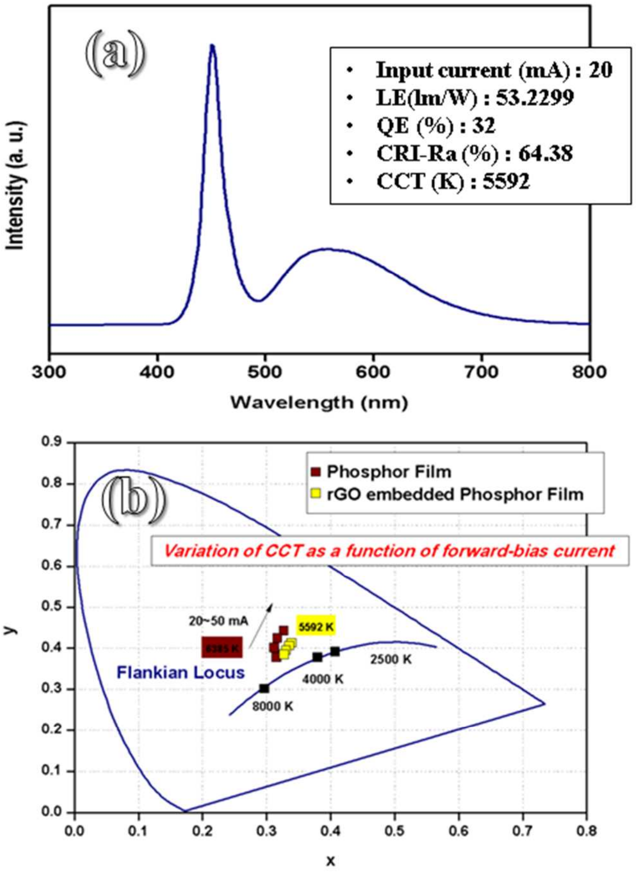

Figure 4. (a) EL Spectra of rGO-embedded remote phosphor, (b) CIE colour coordinate under 20 to 50 mA of forward-bias current

To obtain the performance of rGO-embedded remote phosphor in a device, the electroluminescence (EL) spectra were analyzed in detail, as shown in Figure 4 (a). This EL spectrum consists of a blue LED chip of 450 nm and rGO-embedded remote phosphor. The colour rendering index (CRI) value of a current of 20 mA was 64.38, and the QE was 32 %. To identify the technical applicability of this white light, CCT was determined from the CIE colour coordinate. Figure 4 (b) presents the Plankian locus. The calculated CCT value of rGO-embedded remote phosphor is 5592 K, which is corresponding to daylight (5500-6000K). With increasing the forward-bias current from 20 to 50 mA, the colour point of white LEDs is shifted upward. The increment of chromaticity coordinates (Δx, Δy) is changed. It is assumed that the colour point with increasing the forward-bias current the same for each LED chips. rGO-embedded remote phosphor is more stable against changes in forward-bias current than conventional remote phosphor, which is attributed to the small thermal quenching in rGO-embedded remote phosphor.

To identify the effect of temperature on the photoluminescence, the rGO-embedded remote phosphor was compared to the conventional remote phosphor. Figure 5 (a) indicates the thermal camera image of conventional one. It indicates the average temperature is 92.5 ^{o}C. However, rGO-embedded remote phosphor shows the better average temperature about 83.2 ^{o}C than conventional one. This phenomenon can be explained as the properties of graphene materials. Graphene is a one-atom thick layer, which exhibits high thermal conductivity and electrical conductivity. For these reasons, graphene can resolve the problem of heat dissipation, to improve device reliability.[11, 12].

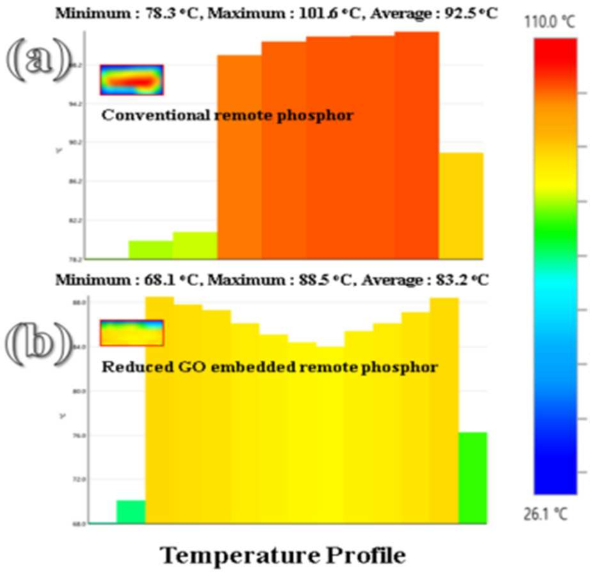

Figure 5. Comparison with thermal camera image (a) conventional remote phosphor, (b) rGO-embedded remote phosphor.

In conclusion, we succeeded in preparing a new remote phosphor using rGO, for high-power LED application. rGO-embedded remote phosphor is a very easy method for making remote phosphor, and is stable, compared with conventional remote phosphor. In addition to the reliability, the thermal stability was improved, due to the high thermal conductivity of the graphene.

This research was supported by Basic Science Research Program through the National Research Foundation of Korea(NRF) funded by the Ministry of Education(NRF-2013R1A1A2059280).

Notes and references

[a] School of Advanced Materials Science & Engineering, Sungkyunkwan University, Suwon 440-746, Republic of Korea. Email: dhyoon@skku.edu, hsjung1@skku.edu

[b] SKKU Advanced Institute of Nanotechnology (SAINT), Sungkyunkwan University, Suwon 440-746, Republic of Korea

[c] Hyosung Corporation, R&D Business Labs, Anyang 431-080, Republic of Korea

[∇]These authors contributed equally to this work.

1 Y. K. Lee, Y. H. Kim, J. Heo, W. B. Im, and W. J. Chung, *Opt Lett.*, 2014, **39**, 4084.
2 J. S. Lee, S. Unithrattil, S. Kim, I. J. Lee, H. Lee, and W. B. Im, Opt Lett., 2013, **38**, 3298.
3 Y. Kawano, S. W. Kim, T. Ishigaki, K. Uematsu, K. Toda, H. Takaba, and M. Sato, *Opt Mater Express*., 2014, **4**, 1770.
4 Y. Liu, X. Zhang, Z. Hao, X. Wang, and J. Zhang, *Chem. Commun.*, 2011, **47**, 10677.

5 J. Y. Han, W. B. Im, G. Y. Lee, and D. Y. Jeon, *J. Mater. Chem.*, 2012, **22**, 8793.

6 K. J. Chen, B. C. Lin, H. C. Chen, M. H. Shih, C. H. Wang, H. T. Kuo, H. H. Tsai, M. Y. Kuo, S. H. Chien, P. T. Lee, C. C. Lin, and H. C. Kuo, *IEEE Photonics J.*, 2013, **5**, 8200508.

7 S. G. Lee, J. Y. Hong, and J. S. Jang, *ACS Nano*., 2013, **7**, 5784.

8 Y. H. Song, E. J. Chung, M. K. Jung, T. Masaki, K. Senthil, S. J. Lee, J. S. Yoo, and D. H. Yoon, *Mater. Lett.*, 2014, **116**, 337.

9 Y. Xu, H. Bai, G. Lu, C. Li, and G. Shi, *J. Am. Chem. Soc.*, 2008, **130**, 5856.

10 W. Q. Chen, D. S. Jo, Y. H. Song, T. Masaki, and D. H. Yoon, *J. Lumin.*, 2014, **147**, 304.

11 J. Y. Hong, and J. S. Jang, *J. Mater. Chem.,* 2012, **6**, 8179.

12 T. H. Han, Y. B. Lee, M. R. Choi, S. H. Woo, S. H. Bae, B. H. Hong, J. H. Ahn, and T. W. Lee, *Nat. Photonics*., 2012, **6**, 105.